J.D. Irish, S.T. Craig and P.J. Valliant, “Preliminary Fission-Product and Post-Irradiation Examination Results from the BTF-105B LOCA/LOECC Test,” Proc. 6th International Conference on CANDU Fuel, Niagara Falls, Ontario, Canada, 1999 September 26-29, ISBN 0-919784-64-X, pp. 291-300.

PRELIMINARY FISSION-PRODUCT AND POST-IRRADIATION EXAMINATION RESULTS FROM THE BTF-105B LOCA/LOECC TEST

J.D. IRISH, S.T. CRAIG AND P.J. VALLIANT

Fuel Safety Branch
Reactor Safety Division
AECL, Chalk River Laboratories
Chalk River, Ontario, Canada K0J 1J0

ABSTRACT

BTF-105B was a well instrumented single-fuel-element test that simulated conditions that could be experienced during a LOCA with LOECC in a CANDU reactor. Average fuel temperatures of 1800°C were maintained for 15 minutes. Released fission products were monitored and collected. Destructive examinations of the fuel have been performed. Preliminary fission-product and post-irradiation examination results are presented.

1. INTRODUCTION

The BTF-105B test was conducted in the Blowdown Test Facility (BTF) of the NRU reactor. This CANDU-Owners-Group-sponsored test was designed to study the release, transport and deposition of fission products from a CANDU-type fuel element during a high temperature transient. Experimental data on fission-product release and transport are required for validating safety-related computer models. A single fuel element was subjected to a blowdown from pressurized steam at low reactor power. Power was then increased in steps until fuel temperatures typical of those which would occur following a LOCA (Loss-Of-Coolant Accident) with additional LOECC (Loss-Of-Emergency-Core Cooling) were obtained [1]. Average fuel temperatures of 1800°C were maintained for 15 minutes. The fuel was preconditioned, to be typical of mid-burnup CANDU fuel, by irradiating it to a burnup of 150 MWh/kgU. The fuel stringer was extensively instrumented and good measurements of neutron flux, coolant flow over the fuel element, and sheath and coolant temperatures were obtained. An irradiation of 17 days immediately prior to the test renewed the inventory of short-lived fission products. Fuel element failure occurred 31 minutes after blowdown. Released fission products were monitored and collected. Following the test, the stringer was potted in epoxy to maintain fuel element geometry. This paper presents preliminary fission-product and post-irradiation examination results for the test.

2. FISSION-PRODUCT RESULTS

For the BTF-105B high temperature transient, ten gamma spectrometers, positioned along facility piping, at a grab-sample station, and at the blowdown (or catch) tank, monitored the release and transport of fission products. Post-transient gamma and chemical analyses were used to quantify fission-product release, fission-product retention, and, following facility cleanup, the decontamination factor. Similar analyses were performed on deposition coupons, filters, and aerosol collectors to provide fission-product-transport data.

Fission-product release depends on the inventory in the fuel at the time of fuel failure. Hence, fractional release is used as a measure of fission-product release. The pre-test inventory can be calculated, and post-test measurements on the fuel element can be used to quantify the retained fission products. For the BTF-105B test, the following steps have been completed:

- Gamma spectroscopy data have been analyzed to quantify the isotopes at the monitor points along the facility piping, in the grab-samples, in the aerosol collection system, and on the deposition coupons. Data from the monitor points, collected during the transient, provide a record of the release and transport kinetics.
- Chemical analyses have been performed on the filters from the aerosol collection system.
- Gamma spectra have been used to quantify the decontamination factors and the total releases for those gamma-emitting isotopes that were reliably detected.
- Axial gamma-scans, gamma radiographs, and gamma tomography of the fuel element have shown the location of fuel loss and the axial distribution of some fission products.
- A simple inventory computation has been performed to estimate the inventory at the time of fuel failure, and to permit a preliminary calculation of the fractional releases.

A detailed inventory calculation is required to arrive at final fractional release values. Radial gamma scans of fuel cross-sections will also be done to determine the distribution of ^{137}Cs, ^{106}Ru, and ^{144}Ce. One use of these data will be in determining the retained fission-product inventory.

2.1 Determining the Fission-Product Release.

Deposition on Blowdown Line

The coolant that passed over the fuel was collected in the blowdown tank, and for 1.5 hours following the test an inert gas-flow purged the facility into the blowdown tank. Despite this, large fractions of some isotopes deposited along the facility piping and in the blowdown line filter and were not delivered to the blowdown tank. For I and Cs, more than half of the total release was held up in the facility. Deposited fission products could not be quantified by direct measurement because of the limited number of observation points along the blowdown line. Also, the quantity of fission products flushed into the blowdown tank during the water-flush process significantly exceeded the integrated deposits over the length of the blowdown line. High concentrations of isotopes must have been hidden from the spectrometers.

The total hold-up in the piping was inferred from the change in activity at the blowdown tank as a result of water flushes used to decontaminate the facility. An average decontamination factor, DF, (activity before water flush divided by activity after the water flush) was determined from pre- and post-flush measurements at the observation points. This DF was used to estimate the quantity of fission products that remained in the pipes after the flush. If the DF is large, then this method is insensitive to variations in water-flush effectiveness over the length of the piping.

The facility cleanup was performed four days after the transient; thus, it was possible to measure longer-lived isotopes as the interfering short-lived isotopes decayed. However, at the time of the cleanup, some short-lived isotopes were no longer detectable. ^{134}I, ^{135}I, ^{134}Cs and ^{138}Cs were not reliably observed over this time-span. The total release was calculated from the ratios of these isotopes to other isotopes of the corresponding element (^{131}I, ^{133}I, and ^{137}Cs). Total ^{132}I release was also found in this way because decay correction of ^{132}I requires an accurate measure of its parent, ^{132}Te. The method of ratios to ^{131}I and ^{133}I produced a smaller uncertainty than that obtained by decay correction with the ^{132}Te parent.

Retention in Blowdown Line Filter

The 74 μm wire-mesh full-flow blowdown-line filter was used to trap large particulates. It was situated 6 m upstream of the blowdown tank. Gamma spectrometers monitored the activity at the inlet and outlet of this filter. For deposited I and Cs a factor of four in activity reduction across the filter was observed. Given the possibility of significant deposition in the filter, it was disassembled after water flushing and gamma spectra were obtained for the individual filter elements. The cleanup was effective and <1% of the total release was retained by the filter after the water flush.

Noble Gases

It is assumed that none of the noble gases was retained in the piping and that any noble gas detected in the blowdown line after the transient was due to decay of a deposited parent (e.g. $^{135}I \rightarrow {}^{135}Xe$). The total noble gas release should simply be what was observed in the blowdown tank. For a day following the transient, high activity in the tank prevented the acquisition of spectra; for a month thereafter, useful spectra were collected. Measurements were made through the tank wall, and both liquid and gaseous samples were drawn from the tank, for gamma-counting in a lower background area. Quantifying noble gas release was further aided in that the gaseous samples were free of iodine that obscured the noble gas gamma-ray peaks in spectra obtained from the tank.

Another approach to quantifying noble gas release is to integrate the activity flow in the blowdown line. In practice, gamma emissions from the noble gases became masked by deposited iodine activity, leading to large uncertainties. Additional uncertainty arose from the need to use flowrate, temperature, and pressure to derive the release rate. For ^{85m}Kr, ^{88}Kr, and ^{135}Xe, sufficient data were obtained to allow an average activity flowrate to be estimated from up to five of the monitor positions along the blowdown line.

2.2 Total Releases.

Estimated total fractional releases for BTF-105B are listed in Table 1 along with those for BTF-104 [2]. A detailed WIMS-ORIGEN calculation had been performed to provide the BTF-104 inventory. For this preliminary work on BTF-105, the inventory was found by scaling the BTF-104 inventory by the relative burn-ups and decay times. Provided that more detailed inventory calculations corroborate the present results, the lack of half-life dependence[1], and the lower releases for the non-gaseous isotopes relative to BTF-104, suggest that the pronounced cooling effect (≈150°C) of the five Zircaloy straps surrounding the element [1] may have restricted the release. (The straps were used to hold thermocouples to the fuel element sheath.) Also, the sheath of the BTF-105 element suffered very little damage relative to the BTF-104 sheath. This may have played a role in the lower fractional releases of the less volatile isotopes.

Note that uncertainties associated with the scaling process are not included in Table 1. This uncertainty is expected to be greater for short-lived isotopes which are sensitive to the detailed power-history during the soak irradiation and the transient. Another unaccounted uncertainty is the possible loss of non-gaseous fission products during an unexpected period of reverse flow that occurred at the end of the transient. The considerable variance in the decontamination factors has been incorporated in the uncertainty. The DF values were as follows:

---

[1] A larger fractional release is expected for the longer-lived isotopes because they can diffuse further through the fuel before decaying.

	Average	Minimum	Maximum
I	2.5	2	13
Te	4.1	3.3	13.8
Cs	7.3	4.4	14.1

^{135}Xe flowrates during the transient are plotted in Figure 1 along with the average flowrate used for integrating the total release. Initially five spectrometers detected ^{135}Xe and were in good agreement. As iodine deposits increased, the measurements diverged and ^{135}Xe detection ceased. Consequently, total release as measured at the blowdown tank and by samples taken from the tank are considered more reliable. Integrated activity flowrate values for ^{85m}Kr, ^{88}Kr, and ^{135}Xe are included in Table 1.

3. POST-IRRADIATION EXAMINATION

After the transient, the fuel element was destructively examined in hot cells. Transverse sections were taken at five axial locations as indicated in Figure 2 for metallographic examinations. Coolant flow was downward over the fuel element; therefore, temperatures would have been higher towards the bottom end of the fuel element.

Figure 3 shows the fuel cross-section at 373 mm from the bottom of the element. This figure shows the fuel element, most of the coolant channel and, in the corners, part of the ZrO_2 shroud which surrounded the coolant channel. This area was remote from the area of maximum damage near the bottom of the element. Aside from a crack through the sheath wall, a fairly uniform oxide layer thickness of 80 to 125 μm and a slight ellipticity, the sheath was not severely damaged. The fuel was cracked but none appears to be missing and there was extensive columnar grain growth. This grain growth was observed in a sister element following the initial irradiation and is not a product of the BTF-105B irradiations. All of the thermocouples in the coolant channel at this elevation appear to be in good mechanical condition and show minimal sheath oxidation. For example, see the cross-section through a Ti/Zr/Ta-sheathed thermocouple, shown in Figure 4.

Figure 5 shows the fuel cross-section at 247 mm. The fuel element, coolant channel, and a Zircaloy strap surrounding the element to hold a thermocouple against the fuel sheath are shown. The strap was intact and hadn't shifted from its original position, indicating that it performed its function. The sheath was in reasonably good condition with one through-wall crack. There were columnar grains in the centre. In the equiaxed region close to the boundary with the columnar grains, there is a dark ring in the fuel. This was seen at other elevations but was most pronounced at this elevation. The dark band is an indication that there was steam ingress, causing the UO_2 to become oxidized.

Figure 6 shows the fuel cross-section at 69 mm. About one quarter of the sheath was missing. The remaining sheath had several through-wall cracks and an oxide layer of non-uniform thickness. In the top left hand corner it can be seen that the oxide thickness increased as the area where the sheath was missing is approached, indicating that the sheath was probably oxidized through in this region from the outside. At the ends of the intact sheath (indicated by arrows) there was some oxidation on the inside, indicating that sheath loss occurred while temperatures were still high, allowing steam access to the inner side of the sheath ends.

Gamma radiography identified the region below 20 mm as likely to be the most damaged. Figure 7 shows the fuel cross-section at 20 mm. At this elevation only one quarter of the sheath remained. Again, the oxide layer was much thicker at one end of the sheath fragment than at the other end, approximately the thickness of the wall at one end. There was little or no oxide on the inside of this sheath fragment, indicating that this region of the inside of the sheath was not exposed to steam while the element was at high temperature. Large chunks of fuel were missing. A cross-section through a Ti/Zr/Ta-sheathed thermocouple, shown in Figure 8, indicates that although the Ti was oxidized and cracked, thermocouple integrity was not compromised.

Figure 9 shows the longitudinal cross-section from the bottom 20 mm of the element. This shows extensive damage. Much of the sheath and fuel were missing. The sheath still attached to the element showed an oxide layer on the outer wall but little oxidation on the inside wall, indicating that the inside of the sheath was not exposed to steam for any significant time while it was still hot. There was minimal damage and oxidation in the vicinity of the end cap, indicating that the fuel adjacent to the end cap was well cooled.

Table 2 lists the sheath oxide thicknesses and UO_2 grain sizes for each axial location. Sheath oxidation ranged from minimal at the top of the element to through-wall oxidation at one area near the bottom. Oxide thickness measurements indicated nonuniform circumferential sheath temperatures. This observation agrees with temperature measurements made in the thermal shroud which surrounded the fuel element. At the peak of the transient, the two shroud thermocouples located at the same height but at different circumferential locations indicated temperatures of 955 and 1076°C. The changes in grain sizes relative to those at the same location of a sister element, which had the same preconditioning irradiation are also listed in Table 2. The greatest percentage change in grain size occurred at the mid-radius. This is consistent with a flatter radial temperature distribution during the steam soak irradiation and transient.

In general, there was more sheath remaining around the BTF-105B fuel element after the transient than was the case for the BTF-104 element. As stated previously, this may have contributed to the relatively smaller release of less volatile fission products during the BTF-105B transient.

4. CONCLUSIONS

Fission-product release quantification and fuel element characterization are two important prerequisites for the use of experimental data in the validation of safety-related computer models. In the BTF-105B test, a single fuel element was subjected to the conditions of a LOCA with LOECC. In addition to recording the process conditions, the well instrumented BTF provided fission-product release, and fission-product transport data. Fission-product releases have been quantified and preliminary fractional releases have been calculated.

Post irradiation examinations indicated that the most severe fuel damage was confined to the lowest portion of the fuel element, in agreement with the results obtained from gamma scanning and gamma radiography [1]. The primary failure appears to be due to through-wall oxidation above the bottom end cap. Fuel-element geometry was well perserved, which should simplify the use of the fission-product release data in model validation.

With the fission-product releases quantified and the fuel-element beginning and end-state characterized, the BTF-105B test should prove to be valuable in the validation of fuel performance and fission-product release models.

5. REFERENCES

1. IRISH J.D. et al., "Preliminary Results of the BTF-105B Experiment: An In-Reactor Test of Fuel Behaviour and Fission-Product Release and Transport under LOCA/LOECC Conditions," Proceedings of the 19th Annual Conference of the Canadian Nuclear Society, Toronto, 1998 October 18-21.
2. DICKSON L.W. et al., "The BTF-104 Experiment: An In-Reactor Test of Fuel Behaviour, and Fission-Product Release and Transport Under LOCA/LOECC Conditions," Proceedings of the 4th International Conference on CANDU Fuel, Pembroke, Canada, pp. 3B-1 to 3B-10, 1995 October 1-4.

TABLE 1: ESTIMATED FRACTIONAL RELEASES

	$\tau_{1/2}$	BTF-105B					BTF-104[2]
	(days)	Inventory, Bq	∫ flow, Bq	Release, Bq	± S	(Release ± S)	(Release ± S)
87-Kr	0.053	1.15E13		2.40E12	19%	(21 ± 5)%	(7 ± 2)%
88-Kr	0.118	2.47E13	4.2E12	3.55E12	31%	(14 ± 5)%	(7 ± 2)%
85m-Kr	0.187	8.73E12	3.1E12	2.57E12	22%	(29 ± 7)%	(10 ± 4)%
85-Kr	3919	4.06E10		1.03E10	24%	(25 ± 7)%	(47 ± 6)%
88-Rb	0.012	2.34E13		2.31E12	20%	(10 ± 2)%	
135-Xe	0.38	1.47E13	1.5E12	1.96E12	28%	(13 ± 4)%	(14 ± 2)%
133m-Xe	2.19	1.61E12		2.67E11	32%	(17 ± 6)%	(19 ± 2)%
133-Xe	5.24	4.63E13		7.63E12	113%	(16 ± 19)%	(23 ± 6)%
90-Sr	10629	2.62E11		1.06E07	22%		
134-I	0.037	4.59E13		4.46E12	36%	(10 ± 4)%	
132-I	0.095	3.45E13		5.32E12	29%	(15 ± 5)%	
135-I	0.274	4.59E13		9.92E12	29%	(22 ± 7)%	
133-I	0.867	5.44E13		7.66E12	36%	(14 ± 5)%	(20 ± 5)%
131-I	8.04	1.76E13		2.90E12	32%	(17 ± 6)%	(33 ± 5)%
132-Te	3.26	3.45E13		2.81E11	26%	(0.8 ± 0.2)%	(2.5 ± 0.7)%
138-Cs	0.0224	2.33E13		6.24E11	67%	(3 ± 2)%	
134-Cs	754	2.97E10		3.10E09	27%	(10 ± 3)%	
137-Cs	11020	3.69E11		6.22E10	25%	(17 ± 5)%	(59 ± 5)%
140-Ba	12.75	2.93E13		6.76E09	57%	(0.02 ± 0.01)%	(1.4 ± 0.2)%

Notes: '**S**' is the sample deviation and known uncertainties. 12% uncertainty on the inventory is included.
$\tau_{1/2}$ is the isotope half-life.
∫ **flow** is the integrated activity flowrate in the blowdown line during the transient.

TABLE 2: OXIDE THICKNESS AND GRAIN SIZE MEASUREMENTS

	Average Grain Size (μm) (change[6])			Oxide Thickness		
Identity	Periphery	Mid-Radius	Centre	Clock Position	Sheath Location	(μm)
MET 1	4.5	12	120	5:00	outside surface	370-375
22 mm	(-8%)[7]	(106%)[7]	(48%)[7]	7:00	"	250-265
				8:00	"	220
MET 2	4.8	5.2	11	12:00	outside surface near top of end plug	94
0-22mm				12:00	end plug/sheath weld area	135
				12:00	end opposite end plug end	220
				6:00	outside surface near top of end plug	114
				6:00	outside surface near top of end plug	300
				6:00	end plug/sheath weld area	150-160
				6:00	outside surface end opposite end plug	290
				6:00	inside surface end opposite end plug	45
MET 3	5.5	20	91	12:00	outside surface	110-112
373 mm	(1%)	(135%)	(20%)	2:00	outside surface	150
				3:00	outside surface	90
				5:00	outside surface	125
				6:00	outside surface	110-115
				9:00	outside surface	80-85
MET 5	5.7	19	95	12:00	outside surface near bearing pad	85
247 mm	(10%)	(40%)	(5%)	12:00	outside surface top of bearing pad	20-25
				3:00	outside surface near spacer pad	90-95
				5:00	outside surface near breach in spacer pad weld	125-130
				5:00	outside surface on top of spacer pad	240
				7:00	outside surface near spacer pad	95
				9:00	outside surface near spacer pad	30
				9:00	outside surface top of spacer pad	10-15
MET 6	5.3	13	60	12:00	outside surface	210
105 mm				3:00	outside surface	200
				4:00	outside surface	290
				6:00	outside surface	380-390[1]
				9:00	outside surface	130-180
MET 7	5.1	17	80	12:00	outside surface	135-140[2]
69 mm	(-5%)	(62%)	(8%)	2:00	outside surface	220
				2:00	inside surface	100-110
				3:00	outside surface	320
				3:00	inside surface	220
				3-4:00		[3]
				7:00		[4]
				7-8:00		[5]
MET 1	4.8	11	69	12:00	outside surface	130
44 mm				3:00	outside surface	150
				4:00	outside surface at break	160
				6:00	outside surface	275-370
				7:00	outside surface	320
				7:00	inside surface	60-65
				900	outside surface	250-290

Notes:
1. completely oxidized in some areas
2. up to 165 in some areas
3. completely oxidized
4. split and completely oxidized
5. splitting and completely oxidized
6. The change in grain size is relative to measurements made at similar positions on archive element A13F that received the same preconditioning irradiation as the BTF-105B element.
7. grain size change for MET 1 is based on the grain size measured for the longitudinal section of element A13F.

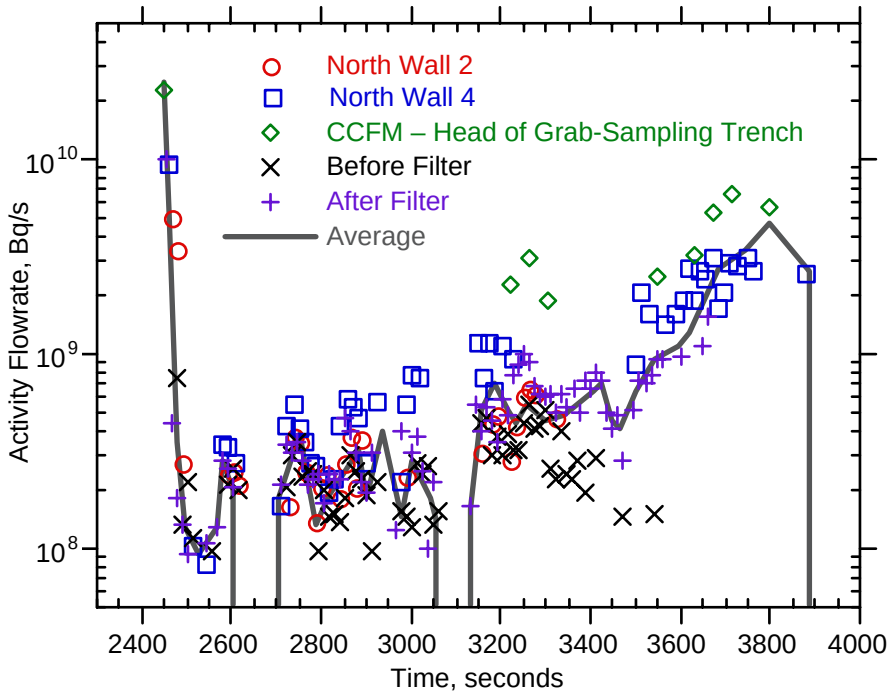

FIGURE 1: ^{135}Xe ACTIVITY FLOWRATE

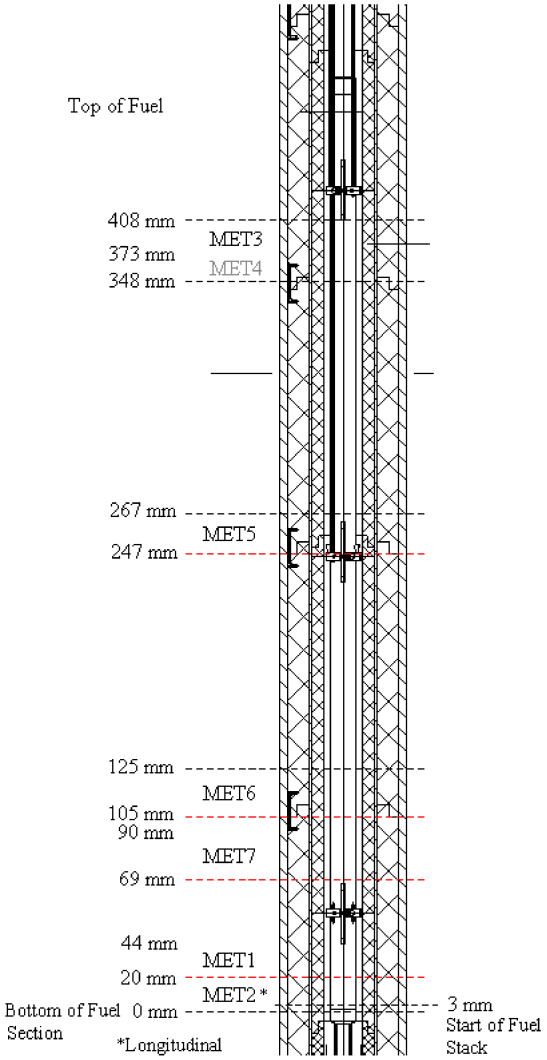

FIGURE 2: CUTTING DIAGRAM

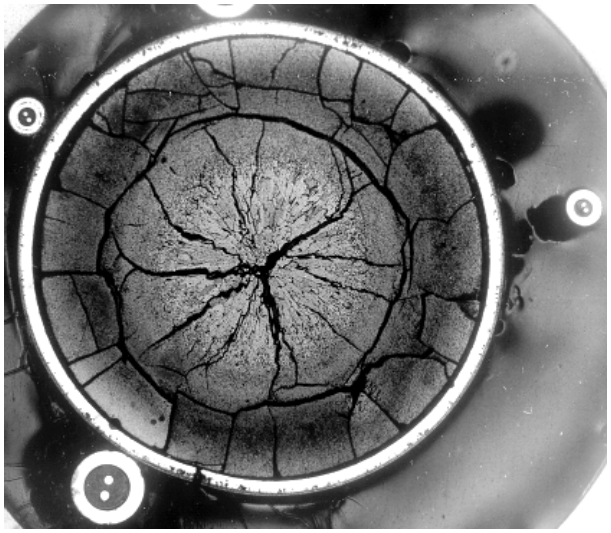

KK19C15 4.8x

FIGURE 3: CROSS-SECTION AT 373 mm

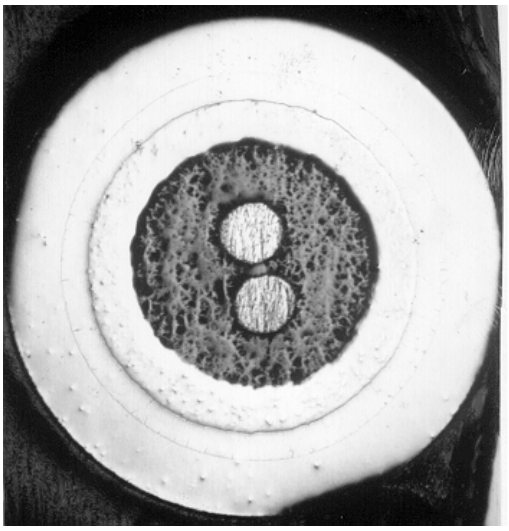

KK19C25 33x

FIGURE 4: THERMOCOUPLE AT 373 mm

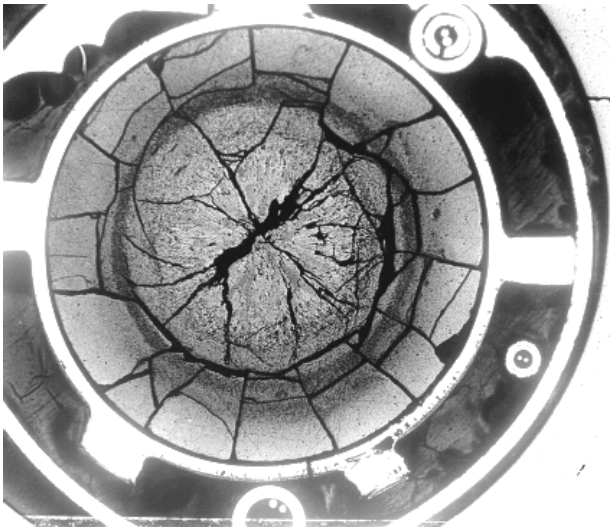

KK19E21 4.8x

FIGURE 5: CROSS-SECTION AT 247 mm

KK19G16 4.8x

FIGURE 6: CROSS-SECTION AT 69 mm

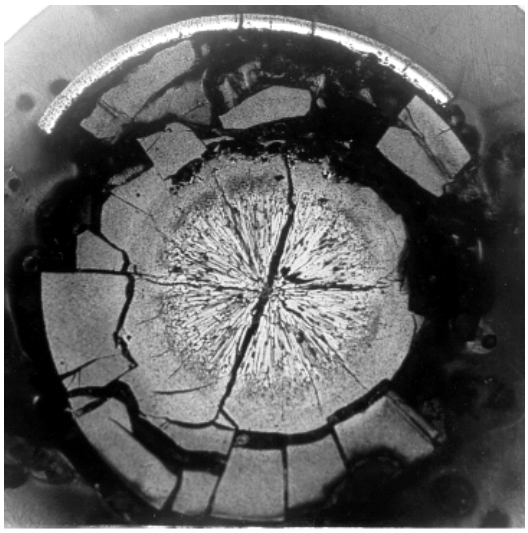

KK19A19 5.2x

FIGURE 7: CROSS-SECTION AT 20 mm

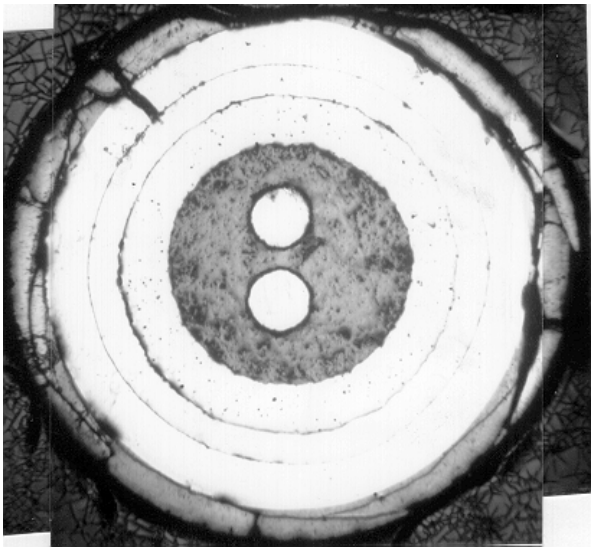

KK19A12 33x

FIGURE 8: THERMOCOUPLE AT 20 mm

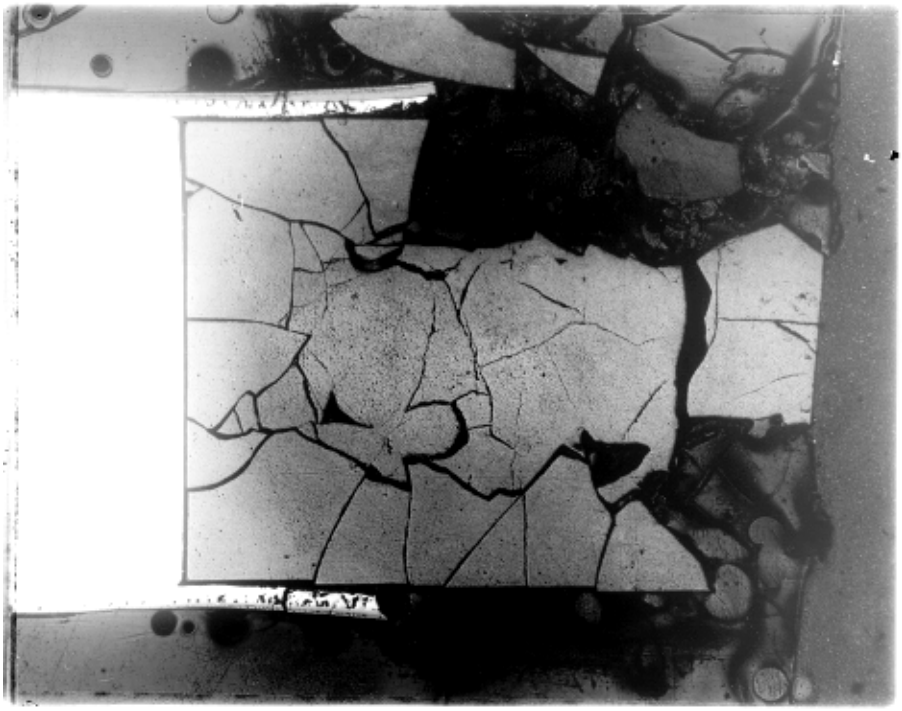

KK19B16 5.2x

FIGURE 9: LONGITUDINAL-SECTION WITH BOTTOM END-CAP